1-5-2016

Oxygen-isotope Variations in Post-glacial Lake Ontario

Ryan Hladyniuk
The University of Western Ontario, r.hladyniuk@austin.utexas.edu

Fred J. Longstaffe
The University of Western Ontario, flongsta@uwo.ca

Oxygen-isotope variations in post-glacial Lake Ontario

Ryan Hladyniuk[1] and Fred J. Longstaffe[1]

[1]Department of Earth Sciences, The University of Western Ontario, London, Ontario, Canada N6A5B7

Corresponding authors, rhladyn@uwo.ca 1-519-619-3857; flongsta@uwo.ca, 1-519-661-3177

Keywords: Lake Ontario, oxygen isotopes, glacial meltwater, Laurentide Ice Sheet, late-Quaternary climate change

Abstract

The role of glacial meltwater input to the Atlantic Ocean in triggering the Younger Dryas (YD) cooling event has been the subject of controversy in recent literature**.** Lake Ontario is ideally situated to test for possible meltwater passage from upstream glacial lakes and the Laurentide Ice Sheet (LIS) to the Atlantic Ocean via the lower Great Lakes. Here, we use the oxygen-isotope compositions of ostracode valves and clam shells from three Lake Ontario sediment cores to identify glacial meltwater contributions to ancient Lake Ontario since the retreat of the LIS (~16,500 cal [13,300 ^{14}C] BP). Differences in mineralogy and sediment grain size are also used to identify changes in the hydrologic regime. The average lakewater δ^{18}O of –17.5 ‰ (determined from ostracode compositions) indicates a significant contribution from glacial meltwater. Upon LIS retreat from the St. Lawrence lowlands, ancient Lake Ontario (glacial Lake Iroquois) lakewater δ^{18}O increased to –12 ‰ largely because of the loss of low-^{18}O glacial meltwater input. A subsequent decrease in lakewater δ^{18}O (from –12 to –14 ‰), accompanied by a median sediment grain size increase to 9 μm, indicates that ancient Lake Ontario received a final pulse of meltwater (~13,000-12,500 cal [11,100-10,500 ^{14}C] BP) before the onset of hydrologic closure. This meltwater pulse, which is also recorded in a previously reported brief freshening of the neighbouring Champlain Valley (Cronin et al., 2012), may have contributed to a weakening of thermohaline circulation in the Atlantic Ocean. After 12,900 cal [11,020 ^{14}C] BP, the meltwater presence in the Lake Ontario basin continued to inhibit entry of Champlain seawater into early Lake Ontario. Opening of the North Bay outlet diverted upper Great Lakes water from the lower Great Lakes causing a period (12,300-8,300 cal [10,400-7,500 ^{14}C] BP) of hydrologic closure in

Lake Ontario (Anderson and Lewis, 2012). This change is demarcated by a shift to higher $\delta^{18}O_{lakewater}$ (~ –7 ‰), driven in part by strong evaporative conditions in the Ontario basin and in part by increasing $\delta^{18}O_{precipitation}$ at this time. The $\delta^{18}O_{lakewater}$ then fluctuated only slightly upon the eventual return of the upper Great Lakes water during the Nipissing phase at 5,800 cal [5,090 ^{14}C] cal BP (Anderson and Lewis, 2012), after which shelly fauna are no longer preserved in the sediment record.

1. Introduction

The timing and volume of glacial meltwater outbursts from large glacial lakes in North America are crucial to understanding their potential role in initiating and/or enhancing climatic changes such as the Younger Dryas (YD) by disrupting thermohaline circulation (THC) in the Atlantic Ocean. Carlson and Clark (2012) and references therein provide an excellent review of the current understanding of late-glacial North American meltwater hypotheses. In short, Broecker et al. (1989) initially proposed that the YD (12,900 cal (calibrated years) [11,020 ^{14}C (radiocarbon)] BP was triggered by a change in meltwater routing of glacial Lake Agassiz from a southern, Mississippi River outlet to an eastern outlet through the Great Lakes (Fig. 1a). Evidence for eastern drainage of glacial Lake Agassiz at that time has remained elusive, as the opening of a suitable eastern outlet has yet to be established by dating (Clark and Carlson, 2012). There is also a lack of geomorphologic evidence for drainage of glacial Lake Agassiz eastward, such as flood deposits and downcut channels (Teller et al., 2005; Voytek et al., 2012). Northwest drainage of glacial Lake Agassiz to the Arctic Ocean at the start of the YD has also been postulated (Murton et al., 2010; Condron and Winsor, 2012; Fahl and Stein, 2012). A re-evaluation by Clark and Carlson (2012) of the optically stimulated luminescence (OSL) dates provided by Murton et al. (2010), however, suggests that the minimum age of a northern outlet was ~12,000 cal [10,240 ^{14}C] BP, much later than the onset of the YD. Carlson et al. (2007) used geochemical proxies preserved in foraminifera collected from the outer St. Lawrence estuary (Fig.1c) to trace freshwater supply to the Atlantic Ocean. These proxies confirmed a freshwater flux into the Atlantic Ocean and Carlson et al. (2007) concluded that an increase in freshwater flux of 0.06 ± 0.02 Sverdrup (Sv) from western Canada (Lake Agassiz) to the St. Lawrence River would have been sufficient to reduce the Atlantic meridional overturning circulation (AMOC). Levac et al. (2015) used microfossils assemblages (foraminifera, diatoms, dinocysts) from cores recovered from the Cabot Strait, Laurentian Channel and Scotian shelf (Fig. 1b) to suggest meltwater drainage via the St. Lawrence River valley to the Atlantic Ocean before/near the onset of the YD. These findings have reignited discussion concerning possible eastward drainage originating from the Great Lakes region.

Other large glacial lakes (Lake Algonquin and Lake Iroquois) also occupied the Great Lakes basin during the period before the YD. Early glacial Lake Algonquin occupied the Huron basin beginning ~13,850 cal [12,000 ^{14}C] BP as ice retreated northward (Fig. 1a) (Eschman and Karrow, 1985). During this time period, there was brief connectivity between the Erie and Huron basins, allowing water to enter glacial Lake Iroquois, which occupied the Ontario Basin at that time (Fig. 1a) (Lewis et al., 1994). Shortly thereafter, glacial Lake Algonquin's water level decreased as water was diverted through the ice-free, isostatically depressed, outlet at Fenelon Falls (Kirkfield-Algonquin phase) and drained directly into the Ontario basin (Fig. 1a) (Eschman and Karrow, 1985; Lewis et al., 2012). As the Fenelon Falls outlet isostatically rebounded above the outlet at Port Huron, glacial Lake Algonquin began to flow southward into the Erie basin, and then onward into glacial Lake Iroquois (Lewis et al., 2012). At ~12,300 cal [10,400 ^{14}C] BP post-glacial Algonquin lakes began draining through a newly open outlet near North Bay, Ontario bypassing the southern Erie and Ontario basins (Fig. 1b) (Lewis et al., 2012). Meltwater routing during the Kirkfield-Algonquin phase (of glacial Lake Algonquin) through glacial Lake Iroquois could have added an additional ~0.1 Sv of freshwater flux to the Atlantic Ocean (Occhietti et al., 2001). Thus, in addition to putative drainage of Lake Agassiz (adding 0.35 Sv of flux; Teller, 1988), contributions from glacial Lake Algonquin and glacial Lake Iroquois could have contributed to suppression of THC and helped to trigger the YD.

Lake Ontario sediments provide a special opportunity to revisit the timing and extent of eastward, glacial meltwater movement that passed through its catchment from various upstream sources (Fig. 1c), especially within the context of the detailed water level history for the Lake Ontario basin presented by Anderson and Lewis (2012). With this objective in mind, we use the oxygen isotopic compositions of ostracodes valves and clam shells, together with sediment characteristics, to test for glacial meltwater contributions to Lake Ontario and its ancient equivalents since the retreat of the LIS (~16,500 cal [~13,300 ^{14}C] BP). We also use the oxygen isotopic compositions of ostracode valves and clam shells in post-glacial sediments to test for Lake Ontario's response to the period of hydrologic closure and associated environmental conditions posited by Anderson and Lewis (2012) and references therein.

1.1 Study Area – Lake Ontario Region

Lake Ontario is the smallest in surface area (slightly less than 19,500 km^2) of the five existing Laurentian Great Lakes (Superior, Michigan, Huron, Erie, Ontario) (Fig. 1c). It measures ~290 km long by ~85 km wide at its widest point and has a maximum water depth of 244 m (McFadden et al., 2005). Lake Ontario shares an international border between Canada (Ontario) and the United States of America (New York).

Lake Ontario's watershed is bounded by the Canadian Shield to the north, the Allegheny Plateau to the south, the Niagara Escarpment to the southwest and west, and the Adirondack Plateau to the east (Hutchinson et al., 1993). The bedrock of the Lake Ontario basin consists of Upper Ordovician shale and limestone, contained within a succession of Cambrian to Carboniferous sedimentary rocks that thickens southward into the Appalachian basin (Hutchinson et al., 1993). At the north and east end of the lake, these sedimentary rocks unconformably overlie the meta-igneous and meta-sedimentary rocks of the Grenville Province of the Canadian Shield (Hutchinson et al., 1993). Two bathymetric ridges (Whitby-Olcott (west) and Scotch Bonnet (east)) subdivide Lake Ontario into three main basins: Niagara (west), Mississauga (central) and Rochester (east). Major water inflow is dominated by the Niagara River to the southwest. It delivers (via Lake Erie) upper Great Lake water to Lake Ontario, which then exits eastward through the St. Lawrence River, presently Lake Ontario's major outlet (Figs. 1b, c). The warm monomictic lake thermally stratifies once per year and has an average water residence time of ~8 years (McFadden et al., 2005).

1.2 Late Quaternary history of the Ontario basin

Correlation of seismic stratigraphy with core lithology and limited geochronology available from various sources, as described below, allows the following description of the sediment record in the Ontario basin. The record began with glacial diamict, possibly a subglacial till composed of deformed glaciolacustrine sediment or flow till. This deposition occurred in the western half of the Ontario basin during retreat of the Port Huron ice lobe at ~16,500 cal [13,300 ^{14}C] BP (Hutchinson et al., 1993). Undisturbed glaciolacustrine deposition, which is characterized by subparallel seismic reflections, began at ~14,000 cal [12,150 ^{14}C] BP (Hutchinson et al., 1993). The Ontario basin was deglaciated earlier than the St. Lawrence River drainage farther to the east as the LIS retreated northward. This caused water to be impounded in the Ontario basin, forming glacial Lake Iroquois, which rose to ~35 m above present Lake Ontario levels (Coakley and Karrow, 1994; Anderson and Lewis, 2012). Growth of glacial Lake Iroquois was regulated by drainage through the Rome Outlet to the Mohawk Valley, with the outflow ultimately travelling to the Atlantic Ocean via the Hudson River valleys (Fig. 1b) (Muller and Prest, 1985, Donnelly et al., 2005).

Glacial Lake Iroquois and its successors persisted until ~13,000 cal [11,100 ^{14}C] BP, at which time further retreat of the LIS made eastward flow of the impounded water possible. The water level of glacial Lake Iroquois water was lowered through several stages ultimately resulting in lake levels that were ~15 m above present lake level in the eastern section of the Ontario basin and below present levels in the west (Coakley and Karrow, 1994; Anderson and Lewis, 2012). The Belleville-Sandy Creek and Trenton-Skinner Creek lake levels of glacial Lake Iroquois were confluent with neighbouring Lake Vermont in the Champlain basin, which flowed to the Atlantic Ocean via the Hudson River valley (Rayburn et al., 2007; Anderson and Lewis, 2012) (Fig. 1b). The last stage (Trenton), which was confluent with Lake Vermont and Lake Candona, formed an extensive body of freshwater throughout the isostatically-depressed upper St. Lawrence River, Lake Champlain and lower Ottawa River valleys and the Lake Ontario basin (Parent and Occhietti, 1988; Rayburn et al., 2007). Additional ice retreat and removal of the ice dam from the lower St. Lawrence valley released this large volume of freshwater to the Gulf of St. Lawrence. Arcuate features across the Ottawa valley, however, blocked that potential meltwater pathway prior to ~12,900 cal [11,000 ^{14}C] BP (Occhietti, 2007). Thus, delivery of lacustrine water from the Great Lakes basin would have required routing through Lake Ontario.

The freshwater that occupied much of lower reaches of the St. Lawrence valley was then replaced by marine water of the Champlain Sea at ~13,000 cal [11,100 ^{14}C] BP (Richard and Occhietti, 2005; Rayburn et al., 2007). The transition to the Champlain Sea involved complex hydrological changes that were recorded by shifting microfaunal assemblages in sediment cores from the Champlain Valley, New York (Rayburn et al., 2011; Cronin et al., 2012). The earliest part of the transition (Marine Phase I) is defined by foraminiferal species (Rayburn et al., 2011). It was followed by periods of abrupt freshening (Freshwater Phase) in which ostracodes emerged and foraminifera disappeared (Rayburn et al., 2011; Cronin et al., 2012). A Transitional Phase then occurred before the onset of Champlain Sea (Marine Maximum at 12,900 cal [11,020 ^{14}C] BP) in which both ostracode and forminifera assemblages co-existed (Rayburn et al., 2011; Cronin et al., 2012). Lake Vermont-Champlain Sea sediments also record signals of glacial meltwater floods, including lower δ^{18}O of marine benthic foraminifera and appearance of freshwater ostracodes (Rayburn et al., 2011; Cronin et al., 2012). While early Lake Ontario was confluent with the Champlain Sea at this time, eastward forcing of freshwater, facilitated by glacial meltwater input to Lake Ontario and isostatic rebound, likely prevented saltwater invasion into early Lake Ontario (Anderson and Lewis, 2012).

The supply of glacial meltwater to early Lake Ontario increased between ~13,000 cal [11,100 ^{14}C] BP and 12,500 cal [10,500 ^{14}C] BP (Anderson and Lewis, 2012). This flow likely included discharge (overflow) from glacial Lake Algonquin (Fig. 1a); this water is assumed to have travelled to Lake Ontario initially by a direct path through the Fenelon Falls outlet in the east and later by a more circuitous route through glacial Lake Algonquin's Port Huron outlet in the west (Fig. 1a) (Eschman and Karrow, 1985; Moore et al., 2000; Anderson and Lewis, 2012).

From 12,300-8,300 cal [10,400-7,500 ^{14}C] BP, flow from the upper Great Lakes (Superior, Michigan, Huron), and potentially Lake Agassiz overflow, was diverted to the North Bay Outlet (Figs. 1b,c), in response to isostatic rebound (Anderson and Lewis, 2012) and ice retreat (Eschman and Karrow, 1985). The outflow then travelled onward via the Ottawa River valley system to the Atlantic Ocean and bypassed the Lake Ontario basin. This rerouting led to hydrologic closure of the lower Great Lakes (Erie and Ontario) and the Lake Ontario water level dropped to the lowest level in its history (Lewis et al., 2012; Anderson and Lewis, 2012). Flow of upper Great Lakes water returned to the lower Great Lakes during the Nipissing phase at 5,800 cal [5,090 ^{14}C] BP (Thompson et al., 2011; Anderson and Lewis, 2012). By then, isostatic rebound had lifted the Lake Huron basin above the outlet at Port Huron, and Lake Ontario water levels began to rise towards present levels (Fig. 1c).

2. Materials and Methods

Three piston cores were collected from Lake Ontario during July 15-17, 2008 by the captain and crew of the Canadian Coast Guard Ship (CCGS) *Limnos*: Core 1335, Mississauga basin; Core 1336, Rochester basin, and Core 1334, Niagara basin (Fig. 2). The cores were cut into ~1 m sections onboard and stored in a refrigerator prior to delivery to the University of Rhode Island, where they were halved longitudinally and visible characteristics (colour, consistency, grain size, sedimentary structures including laminations) noted. Sediment colour was described using the Munsell Soil Color Charts and notation (Munsell Color, 2000). The cores were then shipped to the University of Western Ontario where they continue to be stored at 4°C.

A total of 219 ten-cm sections were extracted from the sampling half of the piston cores. The samples were wet-sieved using cold tap water and a combination of four sieve pans (1.00 mm, 500 μm, 250 μm, 125 μm) to recover ostracodes valves and clams shells; visible organic matter was also collected. The air-dried fossil material was transferred into petri dishes, where the biogenic carbonates were identified and separated by species; ostracodes were counted on the >250 μm sieves. Two species of ostracodes were identified in all three cores, *Candona subtriangulata* and *Fabaeformiscandona caudata*; only adult ostracodes were used for abundance determinations. The ostracodes displayed no macroscopic or microscopic evidence of *post-mortem* transport (e.g., broken/pitted valves), and hence are considered to be autochthonous. Whole clam shells of the *Pisidium* genus were present only in Cores 1334 and 1335 and were less abundant than clam fragments, which were present in all cores at various intervals.

Approximately 0.05 mg of powdered biogenic carbonate was utilized for each oxygen isotopic measurement (five to six ostracode valves were used depending on individual weight; whole clam shells were homogenized when available; when only clam fragments were present, two to three clam shell fragments were utilized). Only undamaged, adult ostracode valves were analyzed to ensure correct identification.

The oxygen-isotope results are presented using the conventional δ-notation:

$$\delta^{18}O = [(R_{sample}/R_{standard})-1] \text{ (in ‰)}$$

where R_{sample} and $R_{standard}$ = $^{18}O/^{16}O$ in the sample and standard, respectively. All δ-values are reported relative to VSMOW, unless otherwise stated. The oxygen-isotope measurements were made in the Laboratory for Stable Isotope Science (LSIS) at the University of Western Ontario, London, Ontario, and were obtained by reaction with orthophosphoric acid (H_3PO_4) at 90°C using a Micromass Multiprep autosampling device coupled to a VG Optima dual-inlet, stable-isotope-ratio mass spectrometer. International standards NBS-19 and NBS-18 were used to provide a two-point calibration curve for the oxygen-isotope compositions relative to VSMOW (Coplen, 1996). Two internal laboratory calcite standards were used to evaluate accuracy and precision of the $\delta^{18}O$ values: WS-1 = +26.28 ± 0.15 ‰ (SD, n=9) and Suprapur = +13.20± 0.07 ‰ (SD, n=24); these results compare well with their accepted values of +26.23 ‰ and +13.20 ‰, respectively.

Values of $\delta^{18}O_{lakewater}$ were calculated using: (1) the ostracode or clam $\delta^{18}O$, after first correcting for any vital effect (*C. subtriangulata* and *F. caudata*, +2.2 ‰; no vital effect correction for *Pisidium* sp. clams; von Grafenstein et al., 1999; Decrouy et al., 2011a, 2011b); (2) an assumed water temperature of 4 °C, and (3) the Friedman and O'Neil (1977) oxygen-isotope geothermometer for the low-Mg calcite – water system.

Mineralogy was determined using powder X-ray diffraction (pXRD) at LSIS, using a Rigaku, high brilliance, rotating-anode X-ray diffractometer equipped with a graphite monochromater and CoKα radiation produced at 45 kV and 160 mA. A total of 85 one-cm thick slices were obtained from the sampling portion of the cores. The samples were freeze-dried, finely ground using a mortar and pestle, and back-packed into an Al sample holder to achieve random orientation. Samples were scanned from 2° to 82° 2θ at a scanning rate of 10° 2θ/min. The abundance of each mineral was estimated using the background-subtracted peak height of its most intense diffraction, except where overlap with other phases existed. The form factor used to adjust for crystallinity differences among minerals was x1, except for the (001) diffractions of kaolinite (×2), chlorite (×2) and illite (×4).

Grain-size analysis was conducted using a Cilas 930e Laser Particle Size Analyzer at the Canada Center for Inland Waters (CCIW), Burlington, Ontario. Forty-six (46) one-cm thick slices from the sampling portion of the cores were freeze-dried and lightly crushed using a mortar and pestle. The homogenized sample was then passed through a 500 μm sieve, and a 0.4 mg sub-sample ultrasonicated for 1 minute in 10 ml of a 0.05 % sodium hexametaphosphate solution in the Cilas sample bucket.

As previously reported by Hladyniuk and Longstaffe (2015), efforts were made to establish an age-depth model anchored by radiocarbon dates. The paucity of dateable terrestrial macrofossils unfortunately precluded such measurements, except for two intervals (Core 1335, 5.25 m; Core 1336, 4.25m) (Fig. 3). In addition to the terrestrial macrofossils, one interval (Core 1334, 5.45m) contained a sufficient abundance of clam shells for radiocarbon-dating; that date was corrected for the hard water effect (HWE) by subtracting 535 ± 15 years (Fig. 3) (Anderson and Lewis, 2012). The dating was performed at the University of Arizona's Accelerator Mass Spectrometer Laboratory, Tuscon, AZ. Radiocarbon dates have been converted to calibrated ages using INTCAL09 (Reimer et al., 2009).

The uncertainty surrounding the HWE correction attached to the radiocarbon date obtained for Core 1334 requires special mention. Anderson and Lewis (2012) used modern mollusc shells to obtain this HWE for Lake Ontario. The HWE in dynamic environments like the one under consideration here, however, can be influenced by numerous factors, including local geology, stratification of meltwater over marine water (Hillaire-Marcel, 1981), and non-equilibration of marine water with atmospheric carbon dioxide (Richard and Occhietti, 2005). Many of these considerations can vary temporally and by specific location (Dyke, 2004). Occhietti and Richard (2003) and Richard and Occhietti (2005), for example, showed that errors associated with HWE correction during the time period of interest here can be on the order of thousands of years in the St. Lawrence Lowlands. In the absence of historical measurements for Lake Ontario, the Anderson and Lewis (2012) HWE correction remains the best available information, but it nonetheless should be accepted with appropriate caution.

Information from previous Lake Ontario core studies was also used to help construct and strengthen the age-depth model (Hladyniuk and Longstaffe, 2015). These data included pollen stratigraphy (Carmichael et al., 1990; McAndrews, 1994; Pippert et al., 1996), seismic stratigraphy (Hutchinson et al., 1993), magnetic properties (Carmichael et al., 1990) and radiocarbon dates (Silliman et al., 1996; Anderson and Lewis, 2012). Notwithstanding this additional information, uncertainties associated with the age-depth model make impossible correlations between glacial meltwater movement through Lake Ontario and other events, for example the timing of the YD, on timeframes shorter than 500 years. Accordingly, we limit our discussion to more general consideration concerning water isotope variations in Lake Ontario and its precursors.

3. Results

3.1 Core descriptions

The bottom sections (>17.0 m) of Cores 1335 and 1336 contain minor and pronounced vertical streaking, respectively. These features suggest sediment disturbance during coring, most probably from suction caused by back-pressure on the piston core barrel. These intervals are not considered further.

Core photographs depicting the major units described below are provided in the Supplementary data; full photographic coverage of the cores is given in Hladyniuk (2014). The basal sections of Cores 1334 (15.0-13.0 m) and 1335 (17.0-12.5 m) consist of massive, grayish-brown (10YR 5/2) sediment containing abundant, light gray, silt balls (Fig. 3). The basal section of Core 1336 (17.0-11.5 m) consists of a grayish-brown (10YR 5/2) sediment package containing weak red (2.5YR 5/2), infrequent, mm-thick, parallel laminations that can be correlated with sediments in Cores 1334 and 1335 (Fig. 3). A sharp contact marks the appearance of thickly laminated sediments at 12.45 m in Core 1334, 11.97 m in Core 1335 and 11.50 m in Core 1336 (lower dashed line in Fig. 4). Upwards in the core, there are infrequent to frequent, mm- to cm-thick, weak red (2.5YR 5/2), parallel laminations that increase in thickness and frequency in the western half of the lake. Massive, grayish brown (10YR 5/2) mud transitioning to infrequent, millimeter-thick, weak red (2.5YR 5/2) parallel laminations appears next in the stratigraphic section. The transition from underlying sediments, which is characterized by cm-thick laminations to thinner, more infrequent laminations, occurs at 10.84 m in core 1334, 9.43 m in core 1335 and 9.00 m in Core 1336. In the west (Niagara basin), Core 1334 transitions from thinly laminated, grayish brown (10YR 5/2) mud to massive, weak red (2.5YR 5/2) mud (9.10 m), overlain by featureless massive, grayish brown (10YR 5/2) mud (8.22-8.06 m) (upper dashed line in Fig. 4). Thinly laminated, grayish brown (10YR 5/2) mud (8.05-6.75 m) was deposited above these massive units. This thinly laminated unit was also deposited in the central, Mississauga basin (Core 1335) of Lake Ontario (9.43-6.20 m), but massive muds were not observed. In the east (Rochester basin), Core 1336 transitions from thinly laminated, grayish brown (10YR 5/2) mud to a massive, featureless grayish brown (10YR 5/2) mud (7.00-4.62 m). A conformable, sharp contact occurs at 6.75 m in Core 1334, 6.20 m in Core 1335 and 4.62 m in Core 1336; sediment characterized by black, iron sulphide streaks is intercalated with dark grayish brown (10YR 4/2) mud.

The basal sediments of Cores 1334 and 1335 correspond to 'Unit B' of Hutchinson et al. (1993) (Fig. 3). A similar mud clast-bearing interval was also described by Pippert et al. (1996), which they termed 'Unit 3'. The contact between the massive, grayish brown (10YR 5/2) unit in Cores 1334 and 1335 and the beginning of the mm-thick parallel laminations is gradational, and marks the transition to 'Unit C' (Hutchinson et al., 1993) (Fig. 3). Unit C also contains a section where laminations increase in frequency and thickness (Hutchinson et al., 1993). This section is followed by sediments showing a decrease in the frequency and thickness of laminations, which has been classified as the earliest stage of 'Unit D' by Hutchinson et al. (1993) (Fig. 3). The conformable, sharp contact, marking the appearance of black, iron-sulphide streaks demarcates the transition from Unit D to 'Unit E' of Hutchinson et al. (1993) ('Unit 1' of Pippert et al., 1996) (Fig. 3). Deposition of this unit continues presently.

3.2 Grain size and mineralogy

Median grain size (diameter at 50 %) in these cores generally increases upwards, but never exceeds ~ 10 μm (Fig. 4). Unit B and the thinly laminated sediments of Unit C have a median grain size of <3.0 μm. The transition to Unit D is marked by a slight increase in median grain size across the lake, and occurs above 10.84 m in Core 1334, above 9.43 m in Core 1335 and above 9.00 m in Core 1336. There are spikes to larger grain sizes within Unit D in all three cores: at 8.90 m and 7.10 m in Core 1334, at 8.10 m in Core 1335, and at 7.30 m in Core 1336. Unit E sediment gradually increases in median grain size up-core to a maximum of 8.0, 9.5 and 6.0 μm from the Niagara to Rochester basin, respectively.

The sediment contains varying abundances of quartz, feldspar (plagioclase, potassium feldspar), clay minerals (kaolinite, illite, chlorite) and carbonates (calcite and dolomite) (Fig. 4). Quartz is usually most abundant, varying from 30 to >80 %. Distinct mineralogical differences occur from west to east in Unit B and the basal section of Unit C. In Core 1334, carbonates are in high abundance (~30 %) from 15.00-13.00 m whereas in the same unit in Core 1335 (17.00-11.97 m) and Core 1336 (17.00-11.50 m), carbonate contents are much lower (~ <5 %). Feldspar and clay mineral abundances also vary from west to east in Unit B and the basal section of Unit C. In Core 1334, feldspar abundance increases sharply to ~25 % at 12.9 m from ≤5 % in the underlying interval (14.0-13.0 m). Feldspar abundance remains at ~15 % in Cores 1335 and 1336 during the same period.

In Unit B and the basal section of Unit C, clay mineral contents increase from west (~20 %) to east (>30 %). Unit D in Core 1334 is marked by an upward decrease in carbonate abundance (~30 to 15 %), whereas in Cores 1335 and 1336 carbonate abundance increases upwards from 15 to 30 %. Carbonate abundances in Unit E vary across the lake. In Core 1334, carbonate content decreases relative to unit D (from 20 to <5 %), whereas in Cores 1335 and 1336, carbonate contents increase initially to a maximum of 40 % but then gradually decrease to <5 %. Clay and feldspar contents remain constant in Unit E whereas quartz abundances generally increase upwards.

3.3 Biostratigraphy

Two species of ostracodes, *C. subtriangulata* and *F. caudata*, and *Pisidium* sp. clams (whole) shells were present in Cores 1334 and 1335 and clam shell fragments were present in all cores (Fig. 4). We have defined three biostratigraphic zonations. Zone 1 has *C. subtriangulata* abundances <0.3 valves per gram sediment (v/g), and occurs at >11.10 m in Core 1334, >9.65 m in Core 1335 and >7.50 m in Core 1336. Zone 2 has higher *C. subtriangulata* abundances to a maximum of 1.56 v/g in Core 1334 (7.10 m), 0.96 v/g in Core 1335 (6.25 m) and 1.50 v/g in Core 1336 (5.05 m). Zone 3 contains both ostracode species and clams. There is a marked decline in the abundance of *C. subtriangulata* in Zone 3 along with the sporadic appearance of *F. caudata* (<0.08 v/g) in low abundances. Both whole and fragments of *Pisidium* sp. clam shells appear at 7.80 m in Core 1334 and 6.05 m in Core 1335. Only fragmented clam shells appear in Core 1336 – at 4.45 m. Ostracodes and clam species disappear from the sediment record at 2.8 m in Core 1334, 3.0 m in Core 1335 and 1.6 m in Core 1336.

3.4 Lakewater oxygen-isotope composition

The average $\delta^{18}O_{lakewater}$, as derived from ostracode compositions, is ~ –17.5±0.8 ‰ (SD; n=81) in sediments >10.84 m in Core 1334, >9.43 m in Core 1335 and >9.00 m in Core 1336 (Fig. 4). Variation in $\delta^{18}O_{lakewater}$ increases from west to east: Core 1334, –17.7±0.2 ‰ (SD; n=14); Core 1335, –17.8±0.7 ‰ (SD; n=36); Core 1336, –17.2±0.9 ‰ (SD; n=31). An analysis of variance (ANOVA) of $\delta^{18}O_{lakewater}$ for these intervals showed significant variation among the three cores (*F*-value= 6, *p*-value=0.005). A *post-hoc* Tukey's test found significant variation between Core 1336 and the other two cores (Core 1334; *p*-value=0.03, Core 1335; *p*-value=0.02), but not between Cores 1334 and 1335 (*p*-value=0.1).

The $\delta^{18}O_{lakewater}$ increases by a maximum of ~7 ‰ from 10.45-7.65 m in Core 1334, 9.05-8.45 m in Core 1335, and 8.85-6.85 m in Core 1336. A decrease in $\delta^{18}O_{lakewater}$ then interrupts the overall trend of increasing oxygen isotopic compositions, beginning at 7.45 m in Core 1334, 8.25 m in Core 1335 and 6.65 m in Core 1336.

The increase in $\delta^{18}O_{lakewater}$ resumes following this brief excursion to more negative values (Fig. 4). For ostracodes, the calculated $\delta^{18}O_{lakewater}$ reaches values as high as –9.1 ‰ in Core 1334, –6.7‰ in Core 1335, and –5.9 ‰ in Core 1336. Still higher $\delta^{18}O_{lakewater}$ is recorded by the clams: –4.2‰ in Core 1334, –4.0 ‰ in Core 1335, and –4.5‰ in Core 1336. Modern Lake Ontario, by comparison, has a $\delta^{18}O_{lakewater}$ of –6.6 ‰ (Longstaffe et al., 2011). Clam shells and fragments in Core 1334 initially record similar $\delta^{18}O_{lakewater}$ as ostracodes but trend toward more ^{18}O-rich compositions after the disappearance of ostracodes. In Core 1335, there is an initial ~1 ‰ offset between clam and ostracode $\delta^{18}O_{lakewater}$, which increases up-core to ~2 ‰ by final appearance of both species. Clam shell fragments in Core 1336, which appear later than in Cores 1334 and 1335, exhibit a ~1 ‰ offset between $\delta^{18}O_{lakewater}$, as inferred from clam versus ostracode oxygen isotopic compositions.

4. Discussion

4.1 Glacial period (16,500-13,260 cal [13,300-11,100 ^{14}C] BP)

The lowermost portions of Cores 1334 and 1335 contain sediments (Unit B or Unit 3, following Hutchison et al., 1993 and Pippert et al., 1996, respectively) deposited in the Niagara and Mississauga basins during the retreat of Port Huron ice. Age control for these sediments is difficult to establish because of the absence of dated pollen horizons and the paucity of dateable organic material. In its absence, linear extrapolation below the inferred contact between Units B and C (14,655 cal [12,500 ^{14}C] BP) (Hutchinson et al., 1993) has been used to estimate that the lowermost Unit B sediments recovered in this study are as old as ~16,500 cal [13,300 ^{14}C] BP.

These sediments are characterized by low abundances of *C. subtriangulata*, very fine grain size (<3 μm) and low $\delta^{18}O_{lakewater}$ (<–17 ‰). Traditionally, these sediments have been interpreted as glacial diamict, possibly a subglacial till composed of deformed glaciolacustrine sediment or flow tills associated with the retreating LIS (Hutchinson et al., 1993). The presence of *C. subtriangulata* in these sediments, albeit at low abundances, supports a deformed glaciolacustrine origin for much of Unit B.

There are noteworthy mineralogical differences between the Niagara and Mississauga basin sediments deposited in Unit B (Fig. 4) that point to differences in their sources. The higher proportions of feldspar and clay minerals in the Mississauga basin sediments (Core 1335) likely reflect increased contribution from the Precambrian Canadian Shield. The higher carbonate abundances in Niagara basin Core 1334 (>30 %) relative to Core 1335 (<5 %) likely indicate greater input from glacial Lake Ypsilanti, which was enriched in Paleozoic carbonate detritus originating in both the Erie and Huron basins. At 16,000-15,300 cal [13,140-12,975 ^{14}C] BP, during the Mackinaw interstadial, the LIS retreated farther east into the Ontario basin, which allowed glacial Lake Ypsilanti (Erie basin) to drain through its outlet at the Fort Erie-Buffalo sill and entered the Lake Ontario basin via Niagara Falls (Fig. 1a) (Lewis et al., 2012). This brief period of connectivity between the Erie and Ontario basins allowed ancestral Lake Ontario to receive glacial meltwater and sediment from the carbonate-rich Erie basin.

Ice readvanced after the Mackinaw interstadial, ending the glacial Lake Ypsilanti phase and severing connectivity between the Erie and Ontario basins (Calkin and Feenstra, 1985; Lewis et al., 2012). Ancestral Lake Erie rose to the Lake Whittlesey level and overflowed westward to the Michigan basin from 15,300-14,500 cal [12,975-12,410 ^{14}C] BP (Calkin and Feenstra, 1985; Lewis et al., 2012). Subglacial deposition became dominant in the Ontario basin during this period. The increase in feldspar content in Core 1334 is consistent with glacial sediment from eastern sources. The variability in $\delta^{18}O_{lakewater}$ during this time interval may be related to the instability of the LIS. The variability in Core 1335 (–17.9±0.6 ‰) may indicate incomplete mixing of an irregular meltwater flux from the LIS to the east and north. The short time scale (on the order of weeks) over which an ostracode acquires its oxygen isotope signal from lakewater makes the recording of such a signal possible. While slightly lower $\delta^{18}O_{lakewater}$

variability in Core 1334 (–17.5±0.4 ‰) may suggest that perturbations in meltwater flux were more limited farther from Core 1335, the isotopic differences between the cores are not statistically significant.

Ice remaining from the northeastward retreating LIS blocked any possible flow of meltwater to the St. Lawrence River, thus facilitating formation of glacial Lake Iroquois (~14,000 cal [12,150 ^{14}C] BP). Glacial Lake Iroquois sediments (Unit C) were observed in the cores from all three Lake Ontario basins. The near uniform abundances of *C. subtriangulata* indicate cold (~ 4 °C), dilute (<90 mg/l total dissolved solids), and oxygenated (>5.6 mg/l) benthic conditions (Delorme, 1978; 1989). The low median grain size (<3 μm) reflects deposition in a deep, low energy, lacustrine environment, which is consistent with glacial Lake Iroquois levels having been ~35 m higher than at present (Coakley and Karrow, 1994).

The relative contributions of different glacial meltwater sources (LIS, glacial Lake Algonquin) to glacial Lake Iroquois probably varied over time. From 14,000-13,000 cal [12,150-11,100 ^{14}C] BP, outflow from glacial Lake Algonquin bypassed the Erie basin and flowed directly into glacial Lake Iroquois via the Fenelon Falls Outlet (Anderson and Lewis, 2012) (Figs. 1a, 2). Data for ostracodes from Lake Simcoe and Lake Huron sediments suggest that glacial Lake Algonquin $\delta^{18}O_{lakewater}$ input ranged from –19 to –17.5 ‰ (Bumstead et al., 2009; Macdonald and Longstaffe, 2008). This meltwater, which entered glacial Lake Iroquois via its northeastern inlet, had a short and direct path to outflow through the Mohawk River valley (Figs. 1a, 2). Core 1336 (–18.1±0.7 ‰) is situated very close to the northeastern inlet to Lake Ontario (Fig. 2), unlike Core 1334 (–17.8±0.3) and to a lesser extent, Core 1335 (–16.8±2.0 ‰). The higher variance in $\delta^{18}O_{lakewater}$ recorded by Cores 1335 and 1336 and the overall lower $\delta^{18}O_{lakewater}$ of Core 1336 relative to Core 1334 can be explained by their locations. In this scenario, the larger $\delta^{18}O_{lakewater}$ variations in Cores 1335 reflect a dynamic lacustrine regime mostly resulting from fluctuating contributions from: (i) the west (regional $\delta^{18}O_{precipitation} = -16.5$ ‰; Edwards et al., 1996), (ii) the east-central outlet of glacial Lake Algonquin (–19 to –17 ‰), and (iii) direct LIS runoff (–35 to –25 ‰) (Ferguson and Jasechko, 2015) from immediately to the northeast. The lowest $\delta^{18}O_{lakewater}$ in eastern glacial Lake Iroquois, in particular, likely reflects increased meltwater delivery directly from the LIS, an observation also consistent with higher feldspar and clay abundances in Core 1336 relative to Cores 1334 and 1335 at this time.

The LIS retreat from the St. Lawrence lowland shortly after ~13,260 cal [11,360 ^{14}C] BP led to eastward drainage of glacial Lake Iroquois and lowstand conditions in the Ontario basin (Anderson and Lewis, 2012) that were likely further enhanced by termination of direct glacial meltwater supply from the LIS. These changes coincided with a regional cold/dry period (Lewis et al., 2008). The ensuing rapid increase in $\delta^{18}O_{lakewater}$ from –19 to –12 ‰ (Fig. 4) may be representative of these conditions. If so, the increase in $\delta^{18}O_{lakewater}$ would reflect elimination of direct, LIS, low-^{18}O glacial meltwater input and perhaps some evaporative ^{18}O-enrichment. From the isotopic data alone, it is impossible to rule out an ^{18}O-rich influx from the confluent Champlain Sea at ~12,900 cal [11,000 ^{14}C] BP (Anderson and Lewis, 2012). There is no evidence for marine invasion of Lake Ontario, however, such as extirpation of the salinity-sensitive *C. subtriangulata* or appearance of marine foraminifera or ostracodes.

4.2 Final glacial meltwater influx (13,000-12,500 cal [11,100-10,500 ^{14}C] BP)

The rise in $\delta^{18}O_{lakewater}$ that began at a suggested age of ~13,260 cal [11,360 ^{14}C] BP was not continuous. In particular, $\delta^{18}O_{lakewater}$ in Core 1335 decreased from ~ –12 to –14 ‰ starting at 8.45 m and continued to decrease until 7.05 m (Fig. 4). This decline could reflect a change in the oxygen isotopic composition of regional precipitation and/or increased influx of low-^{18}O glacial meltwater. The first possibility is unlikely. While pollen and wood cellulose records indicate cold and dry conditions at this time, $\delta^{18}O_{precipitation}$ derived from analysis of coeval wood cellulose rose from –17 to –15 ‰ (Edwards and Fritz, 1986; Edwards and McAndrews, 1989; Edwards et al., 1996). In contrast, increased glacial meltwater input from upstream sources (glacial Lake Algonquin) would produce lower $\delta^{18}O_{lakewater}$, a scenario also supported by the spike in median sediment grain size (~2.5 to 9 μm) measured for this time (Fig. 4). Similar decreases in $\delta^{18}O_{lakewater}$ and increases in median grain size are recorded at 7.65 m in Core 1334 and 6.85 m in Core 1336 (Fig. 4).

Anderson and Lewis (2012) reported inundation of ancient Lake Ontario by glacial meltwater at 12,800 cal [10,965 ^{14}C] BP. Its sources and routing into and out of Lake Ontario, however, have been largely unexplored. Glacial meltwater input from glacial Lake Algonquin (Kirkfield phase) via the Fenelon Falls outlet, which established connectivity with the Ontario basin at 13,000 cal [11,110 ^{14}C] BP (Lewis et al., 2012), could account for this interval of lower $\delta^{18}O_{lakewater}$.

The ultimate source of glacial meltwater input into Lake Ontario that caused the decrease in $\delta^{18}O_{lakewater}$ from –12 to –14 ‰ is of interest, given that this time period may coincide with the beginning of the YD. As noted earlier, Broecker et al. (1989)

hypothesized a change in meltwater routing out of glacial Lake Agassiz from southward (Gulf of Mexico) to eastward (Great Lakes Basin) during the YD. Unfortunately, oxygen isotopes do not provide for a clear distinction between meltwater contributions to Lake Ontario from glacial Lake Agassiz versus other glacial lake(s).

The location of the putative outlet for the final pulse of glacial meltwater received by Lake Ontario is equally enigmatic. One possibility is an eastern outlet into the Champlain Valley. Near the onset of the YD (13,100 cal [11,170 ^{14}C] BP), as discussed earlier, Lake Vermont was transitioning to the Champlain Sea before full onset of the Champlain Sea (Marine Maximum at 12,900 cal [11,020 ^{14}C] BP) (Rayburn et al., 2011; Cronin et al., 2012). Values of $\delta^{18}O_{ostracode}$ measured by Cronin et al. (2012) for the Freshwater and Transitional phases during the Lake Vermont-Champlain Sea transition are very similar to those recorded in Lake Ontario (–14 to –13 ‰). Based on terrestrial radiocarbon dates and the New England varve record, Rayburn et al. (2011) and Cronin et al. (2012) have attributed these changes to glacial meltwater floods (from 13,100-12,900 [11,170-11,020 ^{14}C] cal BP) originating from glacial Lake Agassiz. Notwithstanding the potentially large errors associated with the age-depth model, the increase in meltwater supply beginning at 13,000 [11,100 ^{14}C] cal BP observed here for the Ontario basin, and its possible contribution to climate change, becomes especially interesting in light of the meltwater influxes reported in the Atlantic Ocean during the onset of the YD (Levac et al., 2015).

The lowering of Ontario basin $\delta^{18}O_{lakewater}$ to –14 ‰ likely lasted until ~12,500 cal [10,500 ^{14}C] BP, but there is no record of meltwater entry into the Champlain Sea from ~12,900 cal [11,020 ^{14}C] BP to 11,400 cal [10,000 ^{14}C] BP. Cronin et al. (2012)

postulated that the impact of freshwater events on Champlain Sea salinity must have been swift and immense, and that return to full marine conditions was rapid. The entry of meltwater pulses of this magnitude into Lake Ontario likely prevented incursion of marine water from the east (Anderson and Lewis, 2012). In the absence of substantial meltwater outflow after 12,900 cal [11,020 ^{14}C] BP, water levels in the Ontario basin likely rose to accommodate the incoming glacial meltwater. The sharp increase in $\delta^{18}O_{lakewater}$ that resumed towards the end of this interval is most simply explained by cessation of low-^{18}O meltwater input.

A more robust age model, supported by paleomagnetic secular variation records, is needed to improve current age control on this postulated meltwater incursion into the Ontario basin. Nonetheless, our current ideas correlate well with the lake-level history provided by Anderson and Lewis (2012) (Fig. 5). While acknowledging the potential errors associated with the current age-depth model, it remains that the only evidence of a meltwater flood/routing event passing through the Ontario basin to the Atlantic Ocean is connected to the initial drawdown of glacial Lake Iroquois (Donnelly et al., 2005) and recorded in Lake Ontario sediment beginning at ~13,260 cal [11,360 ^{14}C] BP.

The subsequent increase in meltwater supply to the Ontario basin from glacial Lake Algonquin, which is associated with a decrease in $\delta^{18}O_{lakewater}$ from –12 to –14 ‰, occurred at ~13,000 cal [11,110 ^{14}C] BP and lasted ~500 years. Within the limitations of the current age-depth model, we note that the earliest part of this decrease in $\delta^{18}O_{lakewater}$ potentially correlates with periods of freshening during the Lake Vermont-Champlain Sea transition phase (Cronin et al., 2012). This may indicate a link between Lake Ontario and the events in the Atlantic Ocean observed by Carlson et al. (2007) and Levac et al.

(2015). The lack of evidence, however, for sustained, freshening of the Champlain Sea after this time period (~12,900 cal [11,020 ^{14}C] BP to 12,500 cal [10,500 ^{14}C] BP) suggests that a large portion of meltwater reaching Ontario basin remained there, and hence would have had little impact on Champlain Sea salinity or thermohaline circulation in the Atlantic Ocean.

4.3 Post-glacial transition and hydrologic closure (12,500-8,300 cal [10,500-7,500 ^{14}C] BP]

Following the final influx of glacial meltwater into Lake Ontario, glacial Lake Algonquin outlets at Port Huron and Fenelon Falls were abandoned and outflow diverted to a newly opened northern outlet near North Bay, Ontario (Eschman and Karrow, 1985). The continuing increase in Ontario basin $\delta^{18}O_{lakewater}$ largely reflects the cessation of meltwater influx (Fig. 4). Values of $\delta^{18}O_{lakewater}$ inferred from ostracode compositions reached as high as –9.8 ‰ in Core 1334, –9.9 ‰ in Core 1335 and –9.0 ‰ in Core 1336 by the time of transition from Units D to E. This lithological transition demarcates the end of glacial influence and dates to ~12,300 cal [10,400 ^{14}C] (Hutchinson et al., 1993; Pippert et al., 1996). At this point Lake Ontario entered closed basin conditions according to Anderson and Lewis (2012); they noted that the lowest water levels were a product of evaporative stress, and lasted until ~10,000 cal [8,880 ^{14}C] BP. The appearance of the black streaks (sulphide) at the transition from Units D to E suggests reducing conditions, perhaps caused by an increased demand for oxygen by organisms (Pippert et al., 1996). Water levels gradually rose after that time as evaporative stress eased, but hydrologic closure persisted until ~8,300 cal [7,500 ^{14}C] BP.

The biostratigraphy and $\delta^{18}O_{lakewater}$ of Ontario basin sediments support Anderson and Lewis' (2012) model (Fig. 5). During the early Holocene (until ~ 8,300 cal [7,500 ^{14}C] BP), southern Ontario was influenced mainly by Arctic air masses over the northward-retreating LIS (Edwards et al., 1996). This Arctic influence produced a cold/dry period in southern Ontario, with relative humidity levels 20% lower than at present (Edwards et al., 1996). Over this time period, $\delta^{18}O_{precipitation}$ in southern Ontario increased from –15 to –11 ‰ (Edwards et al., 1996). Such precipitation compositions in the regional watershed would be expected to yield $\delta^{18}O_{lakewater}$ no higher than ~ –12.5 to –8.5 ‰, based on the present spread of ~2.5 ‰ between modern Lake Ontario and precipitation in the region (Longstaffe et al., 2011). Instead, $\delta^{18}O_{lakewater}$ had already increased to a maximum of –7 ‰ (ostracodes) to –6 ‰ (clam shell fragments) (Figs. 4, 5). As such, $\delta^{18}O_{lakewater}$ during this stage of hydrologic closure point to a greater role for evaporative ^{18}O-enrichment than is presently the case.

The rate of increase in $\delta^{18}O_{lakewater}$ appears to slow before the end of hydrologic closure (Figs. 4, 5) at 8,300 cal [7,500 ^{14}C] BP. There is little change in $\delta^{18}O_{lakewater}$ recorded by ostracodes, including *F. caudata* that appeared in Core 1336, and <2 ‰ increase (to –5 ‰) in all cores, based on clams. These results are consistent with the easing of evaporative conditions in the Ontario basin proposed by Anderson and Lewis (2012), as humidity and precipitation levels gradually increased with the onset of warmer conditions.

Low water levels during hydrologic closure were accompanied by appearance of *Pisidium* sp. clams (Cores 1334 and 1335; fragments only in Core 1336) and *F. caudata* in Core 1336, which marks a significant change in the benthic biological community.

This change coincides with hydrologic closure of the Ontario basin and a peak in ostracode productivity in Cores 1334 and 1335. Shallower water is likely key in the emergence of clams (Delorme, 1989). They appeared first in Cores 1334 and 1335, initially as shell fragments, likely transported from shallower water, then as whole shells presumed to have been deposited *in situ* when the basins were at their shallowest (current water depths: Core 1334, 110 m; Core 1335, 192 m).

Clam fragments appear later at the deeper Core 1336 site (current depth, 222 m) (Fig. 4). Shallower water conditions developed later in the vicinity of Core 1336 (current depth, 222 m) than elsewhere in Lake Ontario (Anderson and Lewis, 2012). The appearance of *F. caudata (*and disappearance of *C. subtriangulata)* in Core 1336 suggests that bottom waters in this deeper basin became less oxygenated compared to the western portion of the lake. Although not likely anoxic, the Rochester basin was likely experiencing conditions similar to those found in present Lake Erie (Delorme, 1978). Loss of *C. subtriangulata* typically occurs as dissolved oxygen concentrations fall below 5.6 mg/l. Successive years of low dissolved oxygen cause extirpation of *C. subtriangulata* because of its relatively long life cycle (1 year) and its inability to reach maturity and lay eggs (Delorme, 1978). *F. caudata*, by comparison, has lower minimum dissolved oxygen requirements (2.3 mg/l). Its shorter life cycle (3 to 4 weeks) and associated egg production ensures proliferation for several generations (Delorme, 1978).

In Core 1334, the first clams record $\delta^{18}O_{lakewater}$ similar to coexisting ostracodes. Clams in Cores 1335 and 1336, however, have higher $\delta^{18}O_{lakewater}$ (by 1 to 2 ‰) than ostracodes from the same intervals. These differences could point to the onset of monomictic conditions in ancient Lake Ontario, as has been inferred previously from the carbon isotopic compositions of these fauna (Hladyniuk and Longstaffe, 2015). Clams may have grown in shallower water enriched in ^{18}O by evaporation prior to lake overturn and prior to their transport to deeper parts of the basin after death. The *in-situ* ostracode valves, by comparison, carry deeper, bottom-water $\delta^{18}O_{lakewater}$ signatures characteristic of well-mixed conditions.

4.4 Post-Hydrologic Closure (since 8,300 cal [7,500 ^{14}C] BP]

With the continued retreat and eventual collapse of the LIS, southern Ontario became more strongly influenced by marine tropical air masses originating in the Gulf of Mexico. This caused the regional climate to shift from the cold and dry conditions described earlier, to warm and dry (~8,300 to 6,800 cal [7,500 to 6,000 ^{14}C] BP), and then to warm and wet (at ~6,800 cal [6,000 ^{14}C] BP) (Edwards et al., 1996). Lake levels began to increase at ~8,300 cal [7,500 ^{14}C] BP (Anderson and Lewis, 2012). The Nipissing phase at ~5,800 cal [5,090 ^{14}C] BP is typically used to mark the return of upper Great Lakes drainage to Lakes Erie and Ontario (Anderson and Lewis, 2012), as warmer and wetter conditions were fully established. Evaluating these changes isotopically, however, is difficult because suitable samples were not present at these inferred ages. The ostracode record for Core 1336 suggests that $\delta^{18}O_{lakewater}$ was virtually identical to the present value of –6.6 ‰ just before the disappearance of the biogenic carbonate record (Figs. 4, 5). Clam shells continued to record higher $\delta^{18}O_{lakewater}$ (~ –5 ‰) with perhaps even more ^{18}O-rich, shallow water conditions in Core 1335 at ~ 3.5 m. Results for a coexisting *in situ F. caudata* valve at this depth suggest $\delta^{18}O_{lakewater}$ of at least –5 ‰.

The paucity of suitable samples makes it difficult to comment further except in the most general of terms. By the time of the Nipissing phase, climatic and hydrological conditions in the Ontario basin, at least those that are captured by the $\delta^{18}O_{lakewater}$ signal, were not significantly different from the present time. The shelly fauna then disappear from the sediment records examined here at ~3 m in Core 1334, ~2 m in Core 1335 and ~1 m in Core1336 (Fig. 4). Low sedimentation rates likely caused biogenic carbonates to dissolve before they could be buried, an observation supported by a decrease in detrital carbonate contents over this depth interval (Fig. 4).

5. Conclusions

The oxygen isotopic compositions of ostracodes and clams, supplemented by mineralogical and grain-size information, provide insight concerning the extent, duration and origin of glacial meltwater input into ancient Lake Ontario since the beginning of the retreat of the LIS (~16,500 cal [13,300 ^{14}C] BP). Ostracode proxies for $\delta^{18}O_{lakewater}$ (<–17 ‰) from the lowermost sediments in the western and central portions of Lake Ontario confirm a substantial glacial meltwater presence when the LIS was in close proximity (16,000-15,300 cal [13,140-12,975 ^{14}C] BP). Variations in detrital carbonate, clay and feldspar contents between the western and central portions of the Ontario basin indicate connectivity with ancient Lake Erie (glacial Lake Ypsilanti) at this time. Continued low $\delta^{18}O_{lakewater}$ (<–17.5 ‰) coupled with a change in detrital mineralogy and increased variability in $\delta^{18}O_{lakewater}$ mark the end of connectivity with Lake Ypsilanti (15,300-14,500 cal [12,975-12,410 ^{14}C] BP) to the west and dominance of eastern glacial meltwater inputs to the Ontario basin.

Glacial meltwater originating both from glacial Lake Algonquin and directly from the LIS contributed to glacial Lake Iroquois, which was established in the Ontario basin when LIS retreat blocked the Ontario basin's outlet to the St. Lawrence River (14,000-13,260 cal [12,150-11,360 ^{14}C] BP). Generally lower $\delta^{18}O_{lakewater}$ (–18.1±0.7 ‰) in the eastern portion of glacial Lake Iroquois indicates contributions of meltwater from the LIS. More variable $\delta^{18}O_{lakewater}$ (–16.8±2.0 ‰) in the central portion of glacial Lake Iroquois suggests fluctuations in the relative inflows from the east-central outlet of glacial Lake Algonquin, western sources and direct LIS runoff.

Retreat of the LIS from the St. Lawrence valley shortly after 13,260 cal [11,360 ^{14}C] BP led to eastward drainage of glacial Lake Iroquois and successive lowstand conditions marked by an increase in $\delta^{18}O_{lakewater}$ from –19 to –12 ‰, largely caused by the loss of glacial meltwater input. A decrease in $\delta^{18}O_{lakewater}$ from ~ –12 to –14 ‰ shortly thereafter, about the time of the YD, marked entry of a final pulse of glacial meltwater into the Ontario basin, likely from glacial Lake Algonquin. Meltwater entering the Ontario basin beginning at ~13,000 cal [11,110 ^{14}C] BP may have had brief connectivity to the Atlantic Ocean, but after 12,900 cal [11,020 ^{14}C] BP), there is no compelling evidence that this glacial meltwater reached the Atlantic Ocean. The subsequent increase in $\delta^{18}O_{lakewater}$ from ~ –14 to –9 ‰ marks the loss of glacial meltwater input and hydrologic closure of Lake Ontario. This change in conditions and lower lake levels in particular were marked by appearance of *Pisidium* sp. clams and the ostracode species *F. caudata*. Evaporation under cold and dry conditions during this time is indicated by $\delta^{18}O_{lakewater}$ as high as –6 ‰. By the time of the Nipissing phase, conditions in the Ontario basin captured by the $\delta^{18}O_{lakewater}$ signal were not significantly different from the present time (–6.6 ‰).

Acknowledgements

We thank Allan Crowe (Canada Centre for Inland Waters, Environment Canada) for facilitating core sampling, the Captain and crew of the CCGS *Limnos* for core collection, and the staff of the Laboratory for Stable Isotope Science (LSIS) at the University of Western Ontario for assistance with stable isotope analyses. We are grateful to John King (Graduate School of Oceanography, University of Rhode Island) for core images, Francine McCarthy (Brock University) for pollen extraction, and University of Arizona (AMS) laboratory for radiocarbon dates. We especially thank Editor Dr. Claude Hillaire-Marcel, Dr. Eric Carson and an anonymous reviewer for providing insightful feedback that greatly improved this manuscript. Operating funds were provided by a Natural Sciences and Engineering Research Council of Canada Discovery Grant (FJL) and an Ontario Graduate Scholarship (RH). Infrastructure support was provided by the Canada Foundation for Innovation and the Ontario Research Fund (FJL). The research was also made possible in part through additional research time provided through the Canada Research Chairs program. This is LSIS contribution # 333.

References

Anderson, T.W., Lewis, C.F.M., 2012. A new water-level history for Lake Ontario basin: evidence for a climate-driven early Holocene lowstand. Journal of Paleolimology 47, 513–530. doi:10.1007/s10933-011-9551-8

Broecker, W.S., Kennett, J.T., Flower, B.P., Teller, J.T., Trumbore, S., Bonani, G., Wolfli, W., 1989. Routing of meltwater from the Laurentide Ice Sheet during the Younger Dryas cold episode. Nature 341, 318–320. doi:10.1038/341318a0

Bumstead, N.L., Longstaffe, F.J., Macdonald, R.A., 2009. The paleolimnology of Lake Simcoe: oxygen-isotope compositions of ostracodes. 11th International Paleolimnology Symposium, Guadalajara, Mexico, December 15-18, 2009.

Carlson, A.E., Clark, P.U., Haley, B.A., Klinkhammer, G.P., Simmons, K., Brook, E.J., Meissner, K.J., 2007. Geochemical proxies of North American freshwater routing during the Younger Dryas cold event. Proceedings of the National Academy of Sciences 104, 6556–6561.

Carlson, A. E., Clark, P.U., 2012. Ice sheet sources of sea level rise and freshwater discharge during the last deglaciation. Reviews of Geophysics 50, RG4007. doi:10.1029/2011RG000371.

Carmichael, C.M., Mothersill, J.S., Morris W.A., 1990. Paleomagnetic and pollen chronostratigraphic correlations of the late glacial and postglacial sediments in Lake Ontario. Canadian Journal of Earth Sciences 27, 131–147. doi:10.1139/e90-011

Calkin, P.E., Feenstra, B.H., 1985. Evolution of the Erie-basin Great Lakes. In: Karrow, P.F., Calkin, P.E., (Eds.), Quaternary Evolution of the Great Lakes. Geological Association of Canada Special Paper 30, pp. 149–170.

Coakley, J.P., Karrow, P.F., 1994. Reconstruction of post-Iroquois shoreline evolution in western Lake Ontario. Canadian Journal of Earth Sciences 31, 1618–1629. doi: 10.1139/e94-143

Condron, A., Winsor, P., 2012. Meltwater routing and the Younger Dryas. Proceedings of the National Academy of Sciences 109, 19928–19933. doi: 10.1073/pnas.1207381109

Coplen, T.B., 1996. New guidelines for reporting stable hydrogen, carbon, and oxygen isotope ratio data. Geochimica et Cosmochimica Acta 17, 3359–3360. doi: 10.1016/0016-7037(96)00263-3

Cronin, T.M., Rayburn, J.A., Guilbault, J.-P., Thunell, R., Franzi, D.A., 2012. Stable isotope evidence for glacial lake drainage through the St. Lawrence Estuary, eastern Canada, ~13.1–12.9 ka. Quaternary International 260, 55-65. doi:10.1016/j.quaint.2011.08.041

Decrouy, L., Vennemann, T.W., Ariztegui, D., 2011a. Controls on ostracod valve geochemistry, Part 1: Variations of environmental parameters in ostracod (micro-) habitats. Geochimica et Cosmochimica Acta 75, 7364–7379. doi:10.1016/j.gca.2011.09.009

Decrouy, L., Vennemann, T.W., Ariztegui, D., 2011b. Controls on ostracod valve geochemistry: Part 2. Carbon and oxygen isotope compositions. Geochimica et Cosmochimica Acta 75, 7380–7399. doi:10.1016/j.gca.2011.09.008

Delorme, L.D., 1978. Distribution of freshwater ostracodes in Lake Erie. Journal of Great Lakes Research 4, 216–220.

Delorme, L.D., 1989. Methods in Quaternary ecology #7. Freshwater ostracodes. Geoscience Canada 16, 85–90.

Donnelly, J.P, Driscoll, N.W., Uchupi, E., Keigwin, L.D., Schwab, W.C., Theiler, E.R., Swift, S.A., 2005. Catastrophic meltwater discharge down the Hudson Valley: A potential trigger for the Intra-Allerød cold period. Geology 33, 89–92. doi:10.1130/G21043.1

Dyke, A.S., 2004. An outline of North American deglaciation with emphasis on central and northern Canada. In: Ehlers, J., Gibbard, P.L. (Eds.), Quaternary Glaciations — Extent and Chronology, part II. North America. Developments in Quaternary Science 2, pp. 373–424.

Edwards, T.W.D., Fritz, P., 1986. Assessing meteoric water composition and relative humidity from ^{18}O and ^{2}H in wood cellulose: paleoclimatic implications for southern Ontario. Applied Geochemistry 1, 715–723.

Edwards, T.W.D., McAndrews, J.H., 1989. Paleohydrology of a Canadian Shield lake inferred from ^{18}O in sediment cellulose. Canadian Journal of Earth Sciences 26, 1850–1859, doi: 10.1139/e89-158

Edwards, T.W.D., Wolfe, B.B., MacDonald, G.M., 1996. Influence of changing atmospheric circulation on precipitation δ^{18}O–temperature relations in Canada during the Holocene. Quaternary Research 46, 211–218. doi:10.1006/qres.1996.0061

Eschman, D.F., Karrow, P.F., 1985. Huron basin glacial lakes: a review. In: Karrow, P.F., Calkin, P.E., (Eds.), Quaternary Evolution of the Great Lakes. Geological Association of Canada Special Paper 30, pp. 79–93.

Fahl, K., Stein, R., 2012. Modern seasonal variability and deglacial/Holocene change of central Arctic Ocean sea-ice cover: new insights from biomarker proxy records. Earth and Planetary Science Letters 351–352, 123–133. doi:10.1016/j.epsl.2012.07.009

Ferguson, G., Jasechko, S., 2015. The isotopic composition of the Laurentide Ice Sheet and fossil groundwater. Geophysical Research Letters 42, 4856–4861. doi: 10.1002/2015GL064106

Friedman, I., O'Neil, J. R., 1977. Compilation of stable isotope fractionation factors of geochemical interest. In: Fleischer, M. (Ed.) US Geological Survey Professional Paper 440-KK. Data of geochemistry, US Government Print Office, Washington, DC, USA, pp. 1–12.

Hillaire-Marcel, C., 1981. Paléo-océanographie isotopique des mers postglaciaires du Québec. Palaeogeography, Palaeoclimatology, Palaeoecology 35, 35–119. doi:10.1016/0031-0182(81)90094-8

Hladyniuk, R., 2014. Late Quaternary paleolimnology of Lake Ontario. The University of Western Ontario – Electronic Thesis and Dissertation Repository (Paper 2401).

Hladyniuk, R., Longstaffe, F.J., 2015. Paleoproductivity and organic matter sources in Late Quaternary Lake Ontario. Palaeogeography, Palaeoclimatology, Palaeoecology 435, 13–23. doi:10.1016/j.palaeo.2015.05.026

Hutchinson, D.R., Lewis, C.F.M., Hund, G.E., 1993. Regional stratigraphic framework of surficial sediments and bedrock beneath Lake Ontario. Géographie Physique Quaternaire 47, 337–335. doi:10.7202/032962ar

Levac, E., Lewis, C.F.M., Stretch, V., Duchesne, K., Neulieb, T., 2015. Evidence for meltwater drainage via the St. Lawrence River Valley in marine cores from the Laurentian Channel at the time of the Younger Dryas. Global and Planetary Change 130, 47–65. doi:10.1016/j.gloplacha.2015.04.002

Leverington, D.W., Mann, J.D., Teller, J.T., 2000. Changes in the bathymetry and volume of glacial Lake Agassiz between 11,000 and 9,300 ^{14}C yr BP. Quaternary Research 54: 174-181. doi:10.1006/qres.2000.2157

Lewis, C.F.M., Moore, J.T.C., Rea, D.K., Dettman, D.L., Smith, A.M., Mayer, L.A., 1994. Lakes of the Huron Basin: their record of runoff from the Laurentide Ice Sheet. Quaternary Science Reviews 13: 891-922. doi:10.1016/0277-3791(94)90008-6

Lewis, C.F.M., King, J.W., Blasco, S.M., Brooks, G.R., Coakley, J.P., Croley II, T.E., Dettman, D.L., Edwards, T.W.D., Heil Jr., C.W., Hubeny, J.B., Laird, K.R., McAndrews, J.H., McCarthy, F.M.G., Medioli, B.E., Moore Jr., T.C., Rea, D.K., Smith, A.J., 2008. Dry climate disconnected the Laurentian Great Lakes. EOS, Transactions American Geophysical Union 89, 541–542.

Lewis, C.F.M., Cameron, G.D.M., Anderson T.W., Heil Jr., C.W., Gareau, P.L., 2012. Lake levels in the Erie Basin of the Laurentian Great Lakes. Journal of Paleolimnology 47, 493–511. doi:10.1007/s10933-012-9578-5

Longstaffe, F.J., Ayalon, A., Bumstead, N.L., Crowe, A.S., Hladyniuk, R., Hornibrook, P.A., Hyodo, A., Macdonald, R.A., 2011. The oxygen-isotope evolution of the North American Great Lakes. Northeastern (46th Annual) and North-Central (45th Annual) Joint Meeting of the Geological Society of America, Pittsburgh, Pennsylvania, USA, March 20-22, 2011, p. 57.

Macdonald, R.A., Longstaffe, F.L., 2008. The Late Quaternary oxygen-isotope composition of southern Lake Huron. Aquatic Ecosystem Health and Management 11, 137–143. doi:10.1080/14634980802097236

McAndrews, J.H., 1994. Pollen diagrams for southern Ontario applied to archeology. In: MacDonald, R.I. (Ed.) Great Lakes Archeology and Paleoecology: Exploring Interdisciplinary Initiatives for the Nineties. Quaternary Sciences Institute, University of Waterloo, Waterloo, pp. 179–195.

McFadden, M.A., Patterson, W.P., Mullins, H.T., Anderson, W.T., 2005. Multi-proxy approach to long-and short-term Holocene climate-change: evidence from eastern Lake Ontario. Journal of Paleolimnology 33, 371–391.

Moore Jr., T.C., Walker, J.G.C., Rea, D.K., Lewis, C.F.M., Shane, L.C.K., Smith, A.J., 2000. The Younger Dryas interval and outflow from the Laurentide ice sheet. Paleoceanography 15, 9–18. doi:10.1029/2006PA001340.

Muller, E.H., Prest, V.K., 1985. Glacial lakes in the Ontario basin. In: Karrow, P.F., Calkin, P.E., (Eds.), Quaternary Evolution of the Great Lakes. Geological Association of Canada Special Paper 30, pp. 211–229.

Munsell Color. 2000. Munsell Soil Color Charts Year 2000 Revised Washable Edition. GretagMacbeth, New Windsor, NY.

Murton, J.B., Bateman, M.D., Dallimore, S.R., Teller, J.T., Yang, Z., 2010. Identification of Younger Dryas outburst flood path from Lake Agassiz to the Arctic Ocean. Nature 464, 740–743. doi:10.1038/nature08954

National Oceanic and Atmospheric Administration Digital Elevation Model (DEM) Discovery Portal website (2015). Retrieved June 15, 2015 from http://ngdc.noaa.gov/mgg/dem/

Occhietti, S., 2007. The Saint-Narcisse morainic complex and early Younger Dryas events on the southeastern margin of the Laurentide Ice Sheet. Géographie Physique Quaternaire 61, 89–117. doi:10.7202/038987ar

Occhietti, S., Parent, M., Shilts, W.W., Dionne, J.-C., Govare, E., Harmand, D., 2001. Late Wisconsinan glacial dynamics, deglaciation and marine invasion in southern Québec. In: Weddle, T.K., Retelle, M.J. (Eds.), Deglacial History and Relative Sealevel Changes, 351. Geological Society of America, Northern New England and Adjacent Canada, Boulder, Colorado, pp. 245–272. Special Paper.

Occhietti, S., Richard, P.J.H., 2003. Effet réservoir sur les âges ^{14}C de la Mer de Champlain à la transition Pléistocène-Holocène: révision de la chronologie de la déglaciation au Québec méridional. Géographie Physique Quaternaire 57, 115–138. doi:10.7202/011308ar

Parent, M., Occhietti, S., 1988. Late Wisconsinan deglaciation and Champlain Sea invasion in the St. Lawrence Valley, Quebec. Géographie Physique et Quaternaire 42, 215–246. doi:10.7202/032734ar

Pippert, R.G., Brown, G.R., Morris, W.A., 1996. Palaeomagnetic chronostratigraphy of Holocene sediments, Niagara basin, Lake Ontario, Canada. Journal of Quaternary Science 11, 217–231. doi:10.1002/(SICI)1099-1417(199605/06)

Rayburn, J.A., Knuepfer, P.L.K., Franzi, D.A., 2005. A series of large, Late Wisconsinan meltwater floods through the Champlain and Hudson valleys, New York, USA, Quaternary Science Reviews 24, 2410–2419. doi:10.1016/j.quascirev.2005.02.010.

Rayburn, J.A., Franzi, D.A., Knuepfer, P.L.K., 2007. Evidence from the Lake Champlain Valley for a later onset of the Champlain Sea and implications for late glacial meltwater routing to North Atlantic. Palaeogeography, Palaeoclimatology, Palaeoecology 246, 62–74. doi:10.1016/j.palaeo.2006.10.027

Rayburn, J.A., Cronin, T.M., Franzi, D.A., Knuepfer, P.L.K., Willard, D.A., 2011. Timing and duration of North American glacial lake discharges and the Younger Dryas climate reversal. Quaternary Research 75, 541–551. doi:10.1016/j.yqres.2011.02.004

Reimer, P.J., Baillie, M.G.L., Bard, E., Bayliss, A., Beck, J.W., Blackwell, P.G., Bronk Ramsey, C., Buck, C.E., Burr, G.S., Edwards, R.L., Friedrich, M., Grootes, P.M., Guilderson, T.P., Hajdas, I., Heaton, T.J., Hogg, A.G., Hughen, K.A., Kaiser, K.F., Kromer, B., McCormac, F.G., Manning, S.W., Reimer, R.W., Richards, D.A., Southon, J.R., Talamo, S., Turney, C.S.M., van der Plicht, J., Weyhenmeyer, C.E., 2009. IntCal09 and Marine09 radiocarbon age calibration Curves, 0–50,000 Years cal BP. Radiocarbon 51, 1111–1150.

Richard, P.J.H., Occhietti, S., 2005. ^{14}C chronology for ice retreat and inception of Champlain Sea in the St. Lawrence Lowlands, Canada. Quaternary Research 63, 353–358. doi:10.1016/j.yqres.2005.02.003

Silliman, J.E., Meyers, P.A., Bourbonniere, R.A., 1996. Record of postglacial organic matter delivery and burial in sediments of Lake Ontario. Organic Geochemistry 24 (4), 463–472. doi:10.1016/0146-6380(96)00041-1

Teller, J.T., 1985. Glacial Lake Agassiz and its influence on the Great Lakes. In: Karrow, P.F., Calkin, P.E., (Eds.), Quaternary Evolution of the Great Lakes. Geological Association of Canada Special Paper 30, pp. 1–16.

Teller, J.T., 1988. Lake Agassiz and its contribution to flow through the Ottawa–St. Lawrence system. In: Gadd, N.R. (Ed.), The Late Quaternary Development of the Champlain Sea Basin, 35. Geological Association of Canada, pp. 281–289. Special Paper.

Teller, J.T., Boyd, M., Yang, Z., Kor, P.S.G., Fard, A.M., 2005. Alternative routing of Lake Agassiz during the Younger Dryas: new dates, paleotopography and a re-evaluation. Quaternary Science Reviews 24, 1890–1905. doi:10.1016/j.quascirev.2005.01.008

Thompson, T.A, Lepper, K., Endres. A.L., Johnston, J.W., Baedke, S.J., Argyilan, E.P., Booth, R.K., Wilcox, D.A., 2011. Mid Holocene lake level and shoreline behavior during the Nipissing phase of the upper Great Lakes at Alpena, Michigan, USA. Journal of Great Lakes Research, 37 (2011) 567-576. doi:10.1016/j.jglr.2011.05.012

von Grafenstein, U., Erlernkeuser, H., Trimborn, P., 1999. Oxygen and carbon isotopes in modern fresh-water ostracod valves: assessing vital offsets and autecological effects of interest for palaeoclimate studies. Palaeogeography, Palaeoclimatology, Palaeoecology 148, 133–152. doi:10.1016/S0031-0182(98)00180-1

Voytek, E.B., Colman, S.M., Wattrus, N.J., Gary, J.L., Lewis, C.F.M., 2012. Thunder Bay, Ontario, was not a pathway for catastrophic floods from Glacial Lake Agassiz. Quaternary International 260, 98–105. doi:10.1016/j.quaint.2011.10.040

Figure captions

Figure 1. Digital Elevation Models (DEM) of the Great Lakes basin. Important inlets, outlets and other locations are labeled. (a) Great Lakes basin and position of the Laurentide Ice Sheet at ~13,260 cal [11,350 ^{14}C] BP (Dyke, 2004). Glacial Lake Agassiz (Lockhart phase) drained through the southern outlet (SO) (Leverington et al., 2000). Later in the Lockhart phase and during the Moorhead phase, glacial Lake Agassiz is postulated to have switched from a southern outlet (SO) to an eastern outlet (EO) flowing to glacial Lake Algonquin (Teller, 1985). Early glacial Lake Algonquin's outlet was at Port Huron (PH), which allowed water to enter glacial Lake Iroquois through Niagara Falls (NF) from the Erie basin. Later, during the Kirkfield-Algonquin phase (of glacial Lake Algonquin), water reached glacial Lake Iroquois through the Fenelon Falls (FF) outlet (Eschman and Karrow, 1985; Muller and Prest, 1985). Outflow from glacial Lake Iroquois travelled through the Mohawk River valley, eventually reaching the Atlantic Ocean (Donnelly et al., 2005). (b) Following the draining of glacial Lake Iroquois around 12,900 cal [11,900 ^{14}C] BP early Lake Ontario became confluent with the neighbouring Champlain Sea that inundated the St. Lawrence valley (Anderson and Lewis, 2012). (c) Present configuration of the Great Lakes. All figures modified from the National Oceanic and Atmospheric Administration data center website (http://ngdc.noaa.gov/mgg/dem/).

Figure 2. DEM of Lake Ontario region showing piston core locations: Core 1334 (43° 24' 23" N and 79° 00' 05" W; water depth, 110.3 m; core length, 17.00 m), Core 1335 (43° 33' 19" N and 78° 09' 01" W; water depth, 192 m; core length, 18.20 m), Core 1336 (43° 30' 28" N and 76°

53’ 07” W; water depth, 221.5 m; core length, 18.41 m). Major inlets and outlets during Lake Ontario’s history are labelled. Figure modified from the National Oceanic and Atmospheric Administration data center website (http://ngdc.noaa.gov/mgg/dem/).

Figure 3. Generalized lithology of the Lake Ontario sediments in Cores 1334, 1335 and 1336. Locations of radiocarbon-dated material are denoted by stars. Sediment colour codes follow Munsell Color (2000).

Figure 4. Depth versus: median grain size; bulk sediment mineralogy (triangles, feldspars; squares, clays; stars, carbonates; filled circles, quartz); ostracode abundances, valves per gram sediment (v/g); and $\delta^{18}O_{lakewater}$ inferred from ostracode valves (open circles, *C. subtriangulata*; stars, *F. caudata*) and clam shells (filled triangles) for Core 1334 (Niagara basin), Core 1335 (Mississauga basin) and Core 1336 (Rochester basin). Lithological unit boundaries (see text) are shown by continuous solid (grey) horizontal lines. Important lithological markers (see text) within units are denoted by dashed (grey) horizontal lines. Braces demarcate biostratigraphic zonations as described in the text.

Figure 5. Lake elevation and $\delta^{18}O_{lakewater}$ versus calibrated age in the main Ontario basin. The thick black line indicates the inferred lake level presented by Anderson and Lewis (2012). Major lake phases are noted at the top of the diagram. Values of $\delta^{18}O_{lakewater}$ inferred from *C. subtriangulata* (triangles) and *Pisidium* sp. clams (circles) are shown for Core 1335, and more generally by the colour gradient from low (blue) to high (orange).

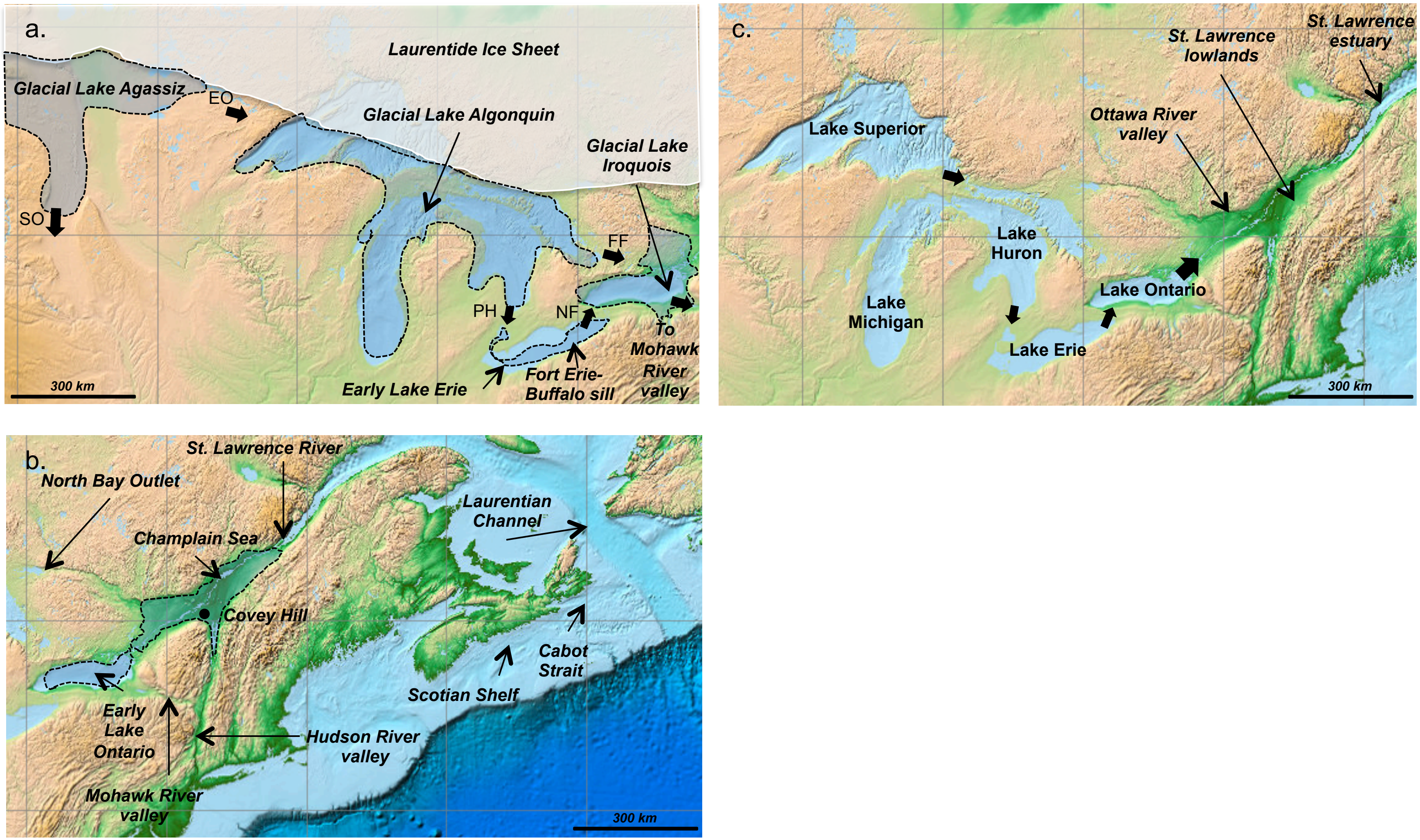

Figure 1.

These figures are a 1-column fitting images (stacked in three). Color only for web version.

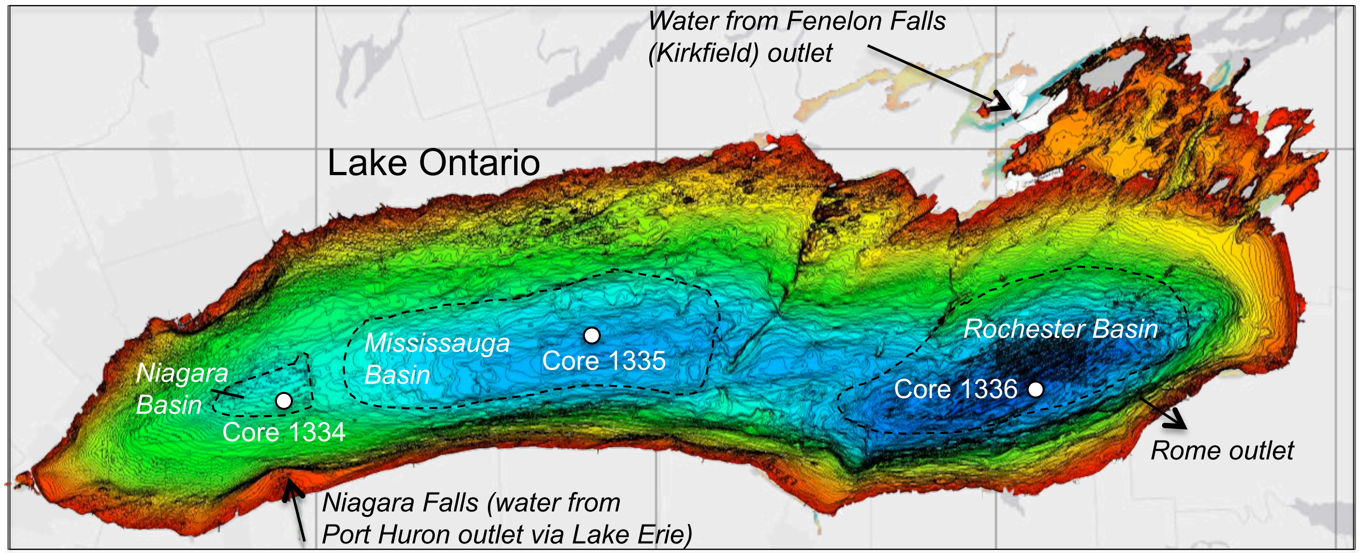

Figure 2.

This figure is a 2-column fitting image. Color only for web version.

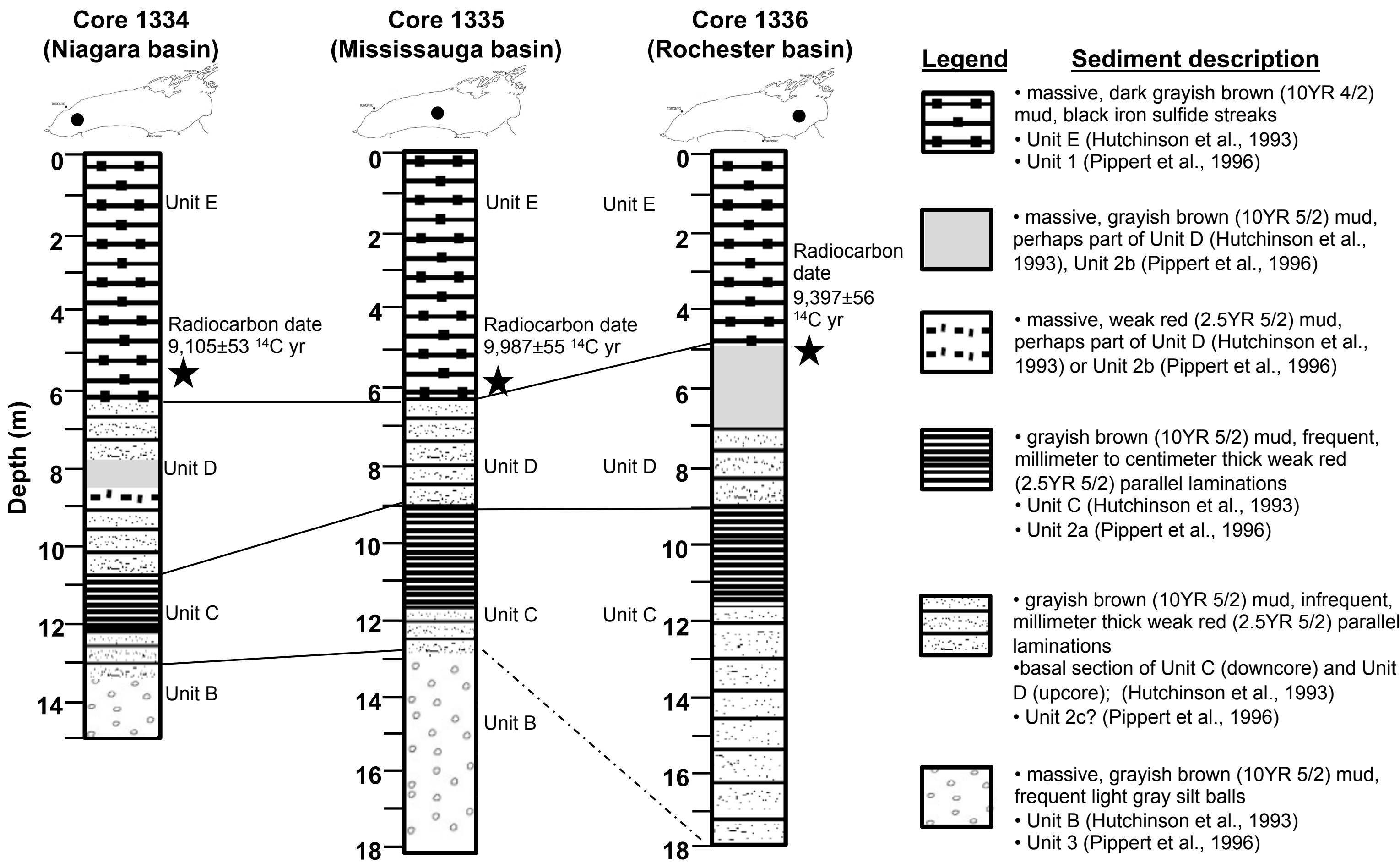

Figure 3.

This figure is a 2-column fitting image.

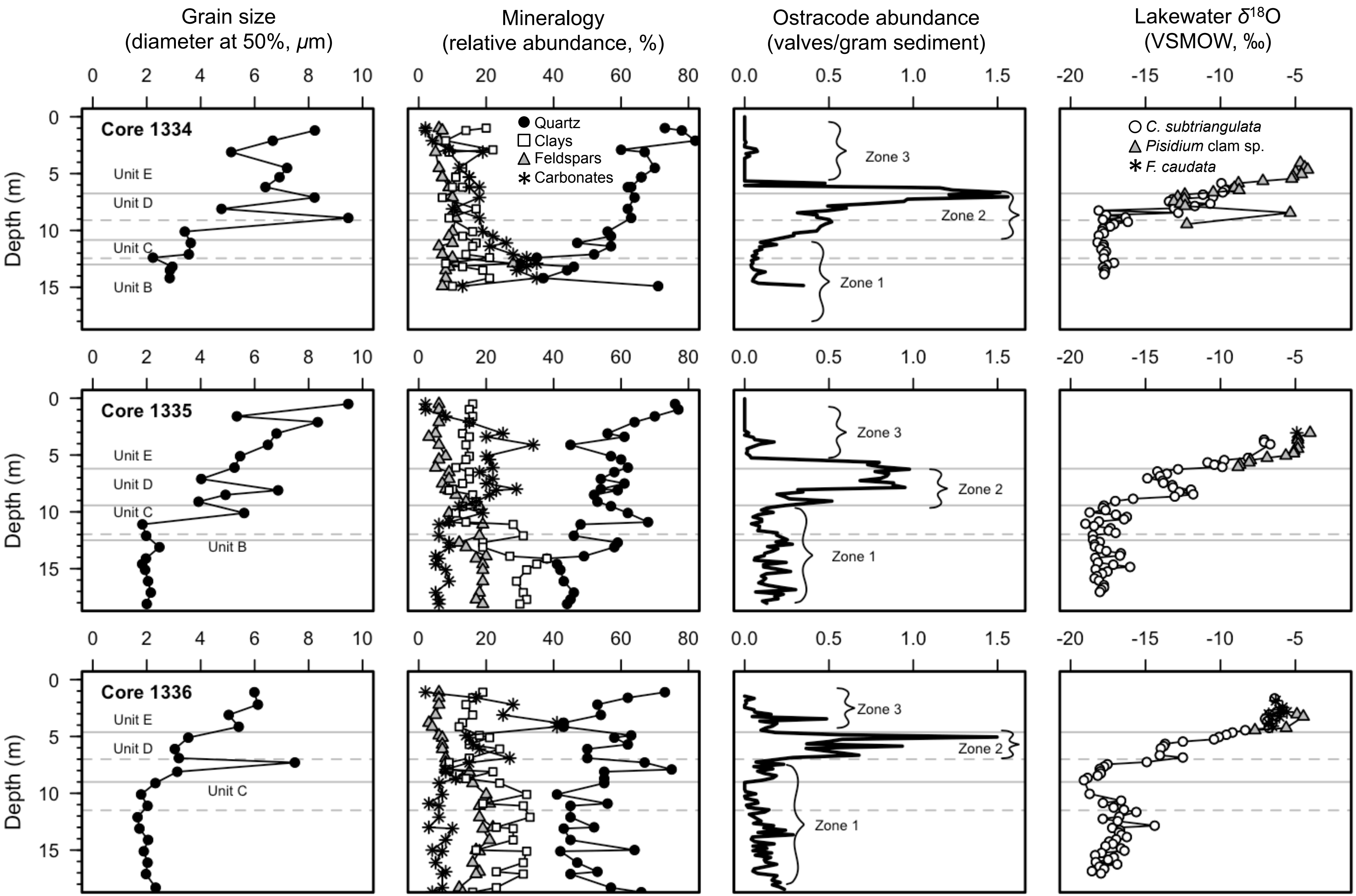

Figure 4. This figure is a 2-column fitting image.

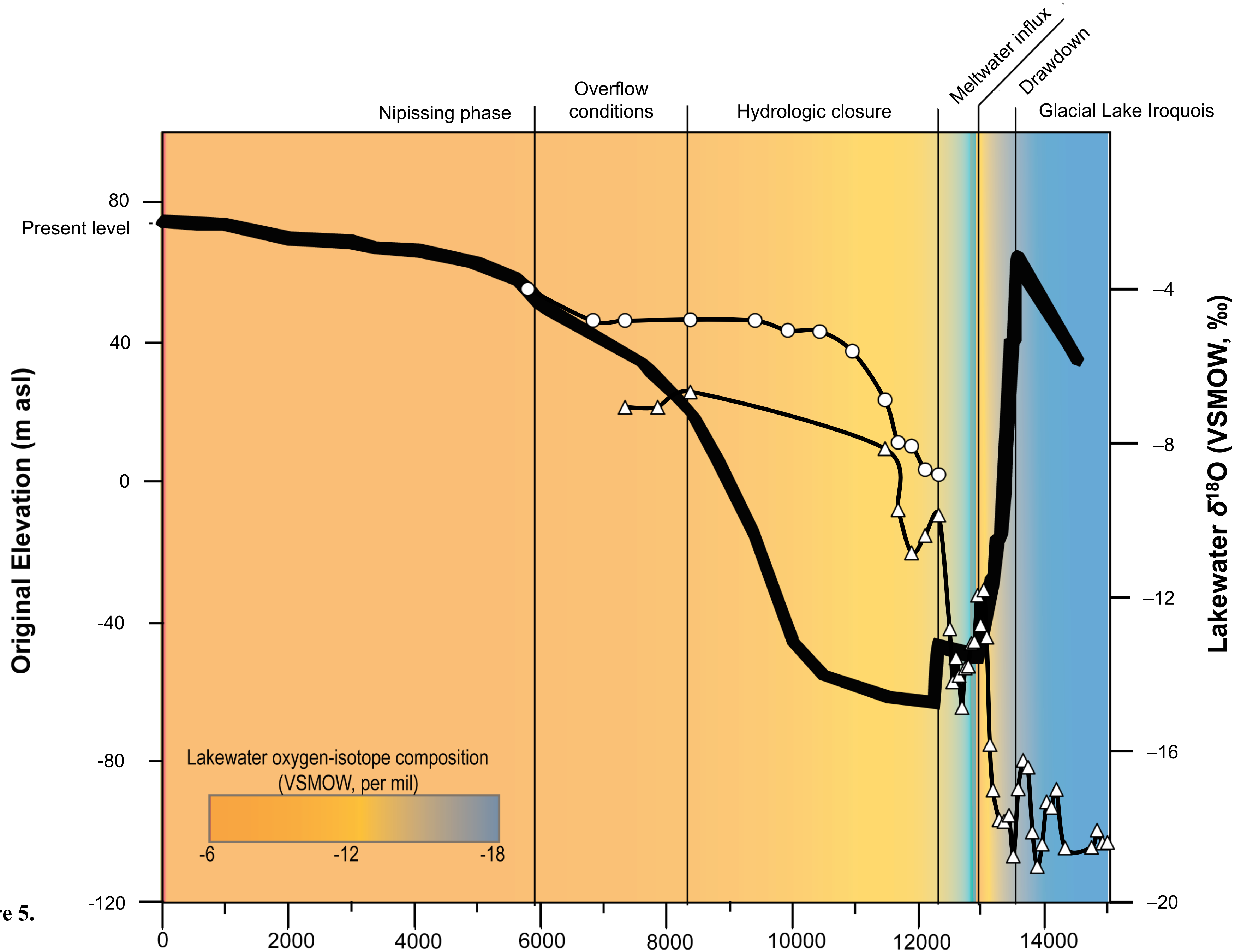

Figure 5.

This figure is a 2-column fitting image.
Color for web version only.